Research Article
doi: 10.1590/01047760202228013077
vol(28), 2022

CERNE

Influence of the addition of microcrystalline cellulose (MMC) on structural properties of cellulose nanofibrils (NFC) suspensions and films

Carmen Fuenmayor [1]✤, Dimas Agostinho da Silva [1], Umberto Klock [1], Elaine Cristina Lengowski [2], Alan Saluto de Andrade [1], Eraldo Antônio Bonfatti Júnior [1], Luzia Rejane Lisbôa Santos [3]

[1] Department of Forestry Engineering and Technology. Federal University of Paraná, Curitiba, Brazil
[2] Faculty of Forestry Engineering. Federal University of Mato Grosso, Cuiabá, Brazil
[3] Laboratory of Advanced Nanomaterials. Center for Strategic Technologies Northeastern, Recife, Brazil

ABSTRACT

Background: In the study of biologically-based materials, nanocelluloses have been showing great prominence and positioned themselves as promising alternatives for the production of different industrialized materials. This polymer has received significant attention recently because it is produced from renewable sources and has unique properties offered by its organic nature and semi-crystalline structure. This work aimed to study the structural properties of suspensions and films by increasing MCC concentration in the form of powder with variations of 5 % (m/m) from 5 % to 30 %.

Results: As expected, incorporating MCC increased the Segal index. The morphological analysis showed an increase in the diameters of the structures (NFC / MCC) in the suspensions when the presence of MCC was more significant, and films with cluster formations were observed. The films showed air permeability. Due to the MCC increase, the surface charge had results close to electrostatically stabilized nanosuspensions. An increase in the resistance to thermal degradation of the films was also observed.

Conclusion: NFC has promising properties for different applications; it provides a film with a stable structure and is resistant to oxygen and tensile stresses. In addition, MCC has excellent potential due to its high crystallinity, structural characteristics, and nature. The increase of the MCC content altered the properties of the suspensions and films produced with NFC, forming a cohesive and resistant film, and influencing the performance of the different properties of the materials evaluated in this study, like air permeability, suspension stability, and thermal resistance.

Keywords: Microcrystalline Cellulose (MCC); Cellulose nanofibrils (NFC); Cellulose nanomaterials

HIGHLIGHTS

Films made with blends of NFC / MCC can be considered impermeable to the air passage;
MCC increments generated results close to electrostatically stabilized suspensions;
The increase in MCC provided increases in the resistance to thermal degradation of the films;
The increase in the crystallinity index was proportional to the percentages of MCC added.

FUENMAYOR, C.; DA SILVA, D. A.; KLOCK, U.; LENGOWSKI, E. C.; DE ANDRADE, A. S.; BONFATTI JÚNIOR, E. A.; SANTOS, L. R. L. Influence of the addition of microcrystalline cellulose (mcc) on structural properties of cellulose nanofibrils (nfc) suspensions and films. CERNE, v.28, n.1, e-103077, doi: 10.1590/01047760202228013077

✤Corresponding author e-mail: carmenfve@gmail.com Submitted: 22/03/2022 Accepted: 17/08/2022

Open Access
CERNE
ISSN 0104-7760
UFLA UNIVERSIDADE FEDERAL DE LAVRAS

INTRODUCTION

Biomass is a source of several chemical substances of industrial interest, among them some polymers with the potential to replace polymers of synthetic origin. In this sense, developing new technologies that seek to extract and use these materials has gained prominence (Hubbe et al., 2017). Synthetic polymers stand out in the production of a variety of disposable products (Khuyen et al., 2021), especially for their characteristics of easy processing, low cost, and good barrier properties; in this context, there is a need to develop new bio-based materials produced with raw materials from renewable, organic, and biodegradable sources (Chu et al., 2020).

In the 1980s, Turbak and Snyder (1983) extracted from cellulose nanostructures as biological, biodegradable materials and, depending on the treatment used, with different characteristics. Highlighted NFC, which has good mechanical and gas barrier properties, characteristics considered promising; however, as it is a hydrophilic material, its use may be limited for some applications (Rol et al., 2019; Konstantinova et al., 2019). On the other hand, MCC is produced especially for use in the pharmaceutical, biomedical, cosmetic, and food industries, transforming it into a material with high crystallinity, hardness, and flexibility that make it attractive for other applications (Hindi, 2017).

Film production from NFC from wood pulp, other fibrous plants, and bacterial cellulose has demonstrated characteristics, properties, and applications for high-tech areas (Su et al., 2017; Fang et al., 2019). It has been considered a new type of special paper, the subject of several pieces of research in the search to direct its use to useful applications in emerging fields (Fang et al., 2019). Nanostructured films as a material have shown outstanding characteristics in the face of a need and demand for cutting-edge and ecologically correct materials (Jiang et al., 2018; Dusastre et al., 2017).

Fuenmayor et al. (2022) studied the tribological performance of NFC films with the addition of MCC and observed a positive correlation of the abrasive wear resistance in the samples concerning the increment of MCC showing results that place them comparable to synthetic films.

Indeed, in the field of research, there is a critical and growing need to expand knowledge and characterize new materials that allow for the prediction of possible applications; in this sense, there was little scientific evidence on the production of nanostructured films composed of NFC and MCC simultaneously, however, several studies through which these two types of materials have been characterized separately. Given this, this work shows its potential since it presents the combined effect of these two types of nanocelluloses.

MATERIAL AND METHODS

Laboratory cellulose nanofibrils (NFC) and commercial microcrystalline cellulose (MCC) was used to prepare the seven suspensions with which the films were later prepared.

NFC was produced from bleached Kraft pulp (elemental chlorine-free sequence) obtained from *Eucalyptus sp.* wood; the pulp exhibited a Kappa number before bleaching of 18, and 1.6 after the last bleaching step reaching a value of 88.8 ISO Bright. The pulp was disintegrated in a blender (power 450 W) for approximately ten minutes before passing to the Supermascolloider MKCA6-2J colloidal mill through 10 passes at 1500 rpm rotation and at a solid concentration (consistency) of 1 %. Several previous studies (Viana et al., 2019; Potulski, 2016; Lengowski et al., 2018) have shown that the fiber dimensions do not change after five passes, but there is a consequent degradation of the cellulose.

The MCC was donated by JRS PHARMA VIVAPUR (Rosenberg, Germany) in the form of a white powder produced from a highly purified pulp, with an average laser diffraction particle size of 45 – 80 µm.

Films production

NFC and MCC were mixed to obtain m:m suspensions by weight of MCC concerning NFC, and the seven treatments were defined according to Table 1, having calculated approximately 150 ml of the suspension for the production of each film.

To ensure that the MCC was dispersed in the mixture, it was dissolved in the necessary water amounts to obtain a NFC / MCC suspension of a solid concentration (consistency) of 1.5 %. Then, each one of the combinations was submitted to mechanical agitation in a beaker for five minutes to formulate seven samples in total and proceed to the films elaboration by laminar deposition on a flat table, forming ten films for each treatment.

Table 1. Treatments and nomenclatures according to MCC / NFC percentages.

Treatments / Nomenclatures	NFC (%)	MCC (%)
FO	100	0
FPC	95	5
FPD	90	10
FPQ	85	15
FPV	80	20
FPY	75	25
FPT	70	30

Microstructural analysis of NFC / MCC suspensions and filmes

For the analysis of the structures in the suspensions, a Transmission Electron Microscope (TEM) model Jeol JEM 1200 EXII was used with a resolution of 0.5 nm (600 thousand X); each suspension was prepared at five ppm diluted in distilled water and dripped onto the surface of the observation screen and transferred to a desiccator for drying at room temperature (Lengowski et al., 2018).

Through the electron micrographs obtained from the TEM, a particle sizing analysis was performed with a sampling intensity of 60 units in an area of 2.62 mm^2, with the help of an image analysis software and a thresholding filter (ImageJ).

The formed (dry) films surfaces were analyzed using a Scanning Electron Microscope (SEM) FEI Quanta 450 FEG, resolution 0.1 nm, HV = 12 kV, Mag = 5 kx, and view field = 55.4 µm. The films were placed on aluminum sample holders with double-sided carbon tape coated with gold.

Physical properties of films

Humidity, thickness, weight, and apparent density

The physical tests of humidity, thickness, weight and apparent density were carried out in a controlled environment (temperature 23 ± 1 °C and relative humidity 50 ± 2 %) following the TAPPI 402om:1994 specifications (TAPPI, 1994). Ten samples per treatment were evaluated. Moisture was determined in the films by the gravimetric method and according to the TAPPI 412om:2016 standard (TAPPI, 2016a). The thickness using the gauge ME-1000 REGMED through the TAPPI 220sp:2016 (TAPPI, 2016b). The grammage was determined following the recommendations of the TAPPI 410om:2019 (TAPPI, 2019) where the films were weighed, and their area was determined. The apparent density was calculated according to the specifications of the TAPPI 220sp:2016 standard (TAPPI, 2016b) calculated by the film weight and thickness ratio.

Air permeability

Using the Gurley method, the amount of time required for a given air volume to pass through the film was measured according to TAPPI 460-om:2016 (TAPPI, 2016c). The recommended time interval for this test is from 5 to 1800 s for 100 mL of air; above this range, it is classified as impermeable material.

Difração de Raios X

The analysis was performed on dry films. The slotted monochromator mode configuration (1, 1, 0.3) was adopted through the X-ray diffractometer equipment XRD-7000 from SHIMADZU operating at 40 kv with a current of 20 mA; rays were collected in the range of 2θ = 3-40° at a speed of 2 °/min using Cu-Kα radiation with a wavelength of λ=0.15418 nm (Lengowski et al., 2018). The data obtained were analyzed with a baseline and correction filter by Fourier transform (20%) to obtain the peaks with the OriginPRO software.

According to French (2020), several diffraction methods are used to analyze the crystallinity of cellulose, and even when there is no consensus regarding which method to apply, the Segal method is the most used (Segal et al., 1959). The crystallinity index was determined by the Segal method.

Chemical characterization

Zeta Potential

The zeta potential analyzes were performed in the Stabino PMX 400 equipment with aliquots of the mixture suspensions in the proportion of 1:100 (m/m) diluted in distilled water. Seven replicates were made for each treatment, with 121 observations in each replicate. The equipment measures the surface charge of the particles, which is directly related to their stability in dispersion.

Fourier Transform Infrared Spectroscopy (FTIR)

Measurements were performed on previously dried films, using a Bomem Michelson MB100 device with 32 scans acquisition, 4 cm^{-1} resolution, in the absorption range between 4000 and 400 cm^{-1}.

Thermal characterization

Thermogravimetric analysis (TGA)

The analyzes were performed using TA Instruments Q50 equipment under conditions of argon atmosphere in a continuous flow of 60 $mL.min^{-1}$. A sample with around 5 mg of sample in platinum crucibles was used at a heating rate of 10 $°C.min^{-1}$, in a temperature range from 25 °C to 600 °C. Usually, an inert or synthetic atmosphere is used for thermal analysis; the gas used (Argon) is an inert gas frequently used for the thermogravimetric analysis of the cellulose (Nurazzi et al., 2021; Huang et al., 2012; Leal et al., 2015; Hameed et al., 2022; Mironova et al., 2019; Monteiro et al., 2012).

Statistical analysis

According to the nature of each test, the following analyzes were carried out: descriptive statistics and/or dispersion for morphology, zeta potential, and physical properties. In addition, it was made a frequency analysis for morphology. For zeta potential and physical properties, a normality test (Kolmogorov-Smirnov and Shapiro-Wilk, respectively) for homogeneity of variance (Levene) and a difference of means test for independent samples (Kruskal-Wallis H for non-homogeneous variances and ANOVA for variances homogeneous). The evaluated properties were considered dependent variables, and as independent variables, the increase in the concentration of MCC in NFC according to the treatments presented in Table 1. The IBM SPSS Statistic 22 tool was used.

RESULTS

Microstructural analysis of NFC / MCC suspensions and filmes

In Figure 1, the MET micrographs for each treatment are shown. From the MET micrographs, an analysis of diametric frequencies was performed, presented in Figure 2, Figure 3 shows part of the SEM micrographs of the surface of the films..

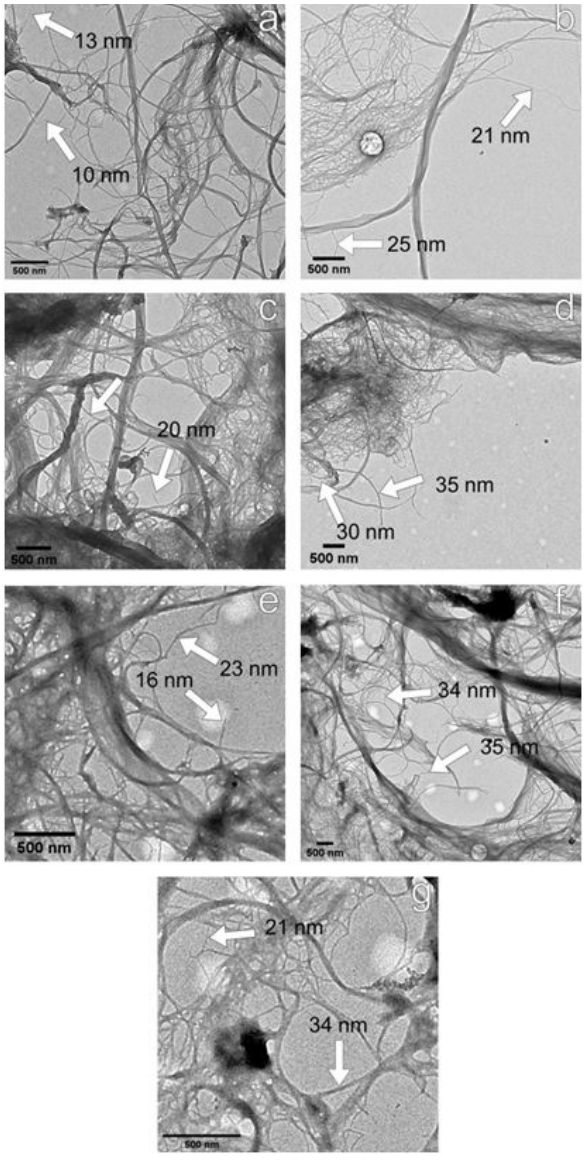

Figure 1. Microstructural analysis (TEM) of NFC / MCC suspensions. a) FO, b) FPC, c) FPD, d) FPQ, e) FPV, f) FPY and g) FPT.

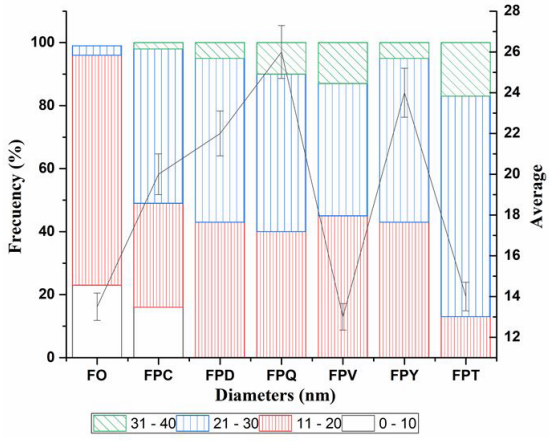

Figure 2. Diametric distribution of NFC / MCC structures in suspensions.

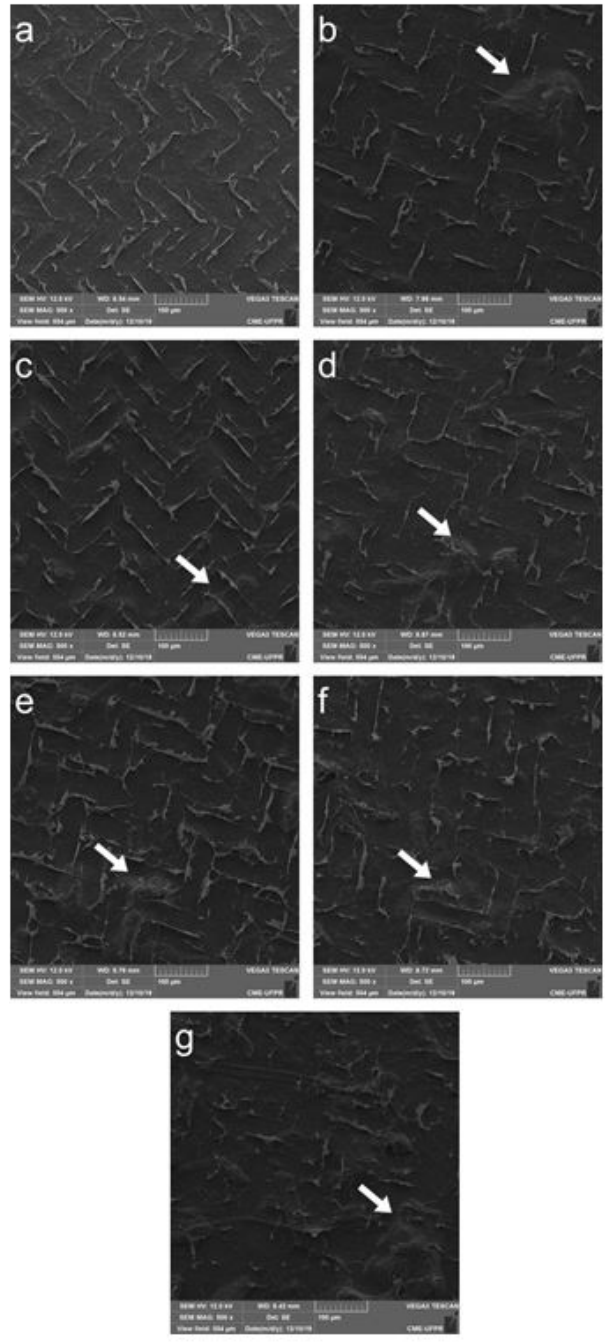

Figure 3. Microstructural analysis (SEM) of NFC / MCC filmes. a) FO, b) FPC, c) FPD, d) FPQ, e) FPV, f) FPY and g) FPT.

Physical properties of films

Humidity, thickness, weight, and apparent density

Moisture and grammage were controlled properties in the laboratory; the grammage had no significant differences between the samples (values between 16.69 g.m^{-2} and 20.3 g.m^{-2}), and the average humidity of the films remained at 9 ± 1 %.

In the case of the thickness (averages between 21.60 µm and 63.60 µm), a maximum value was observed for the film with the highest percentage of MCC addition (FPT) and a minimum value for the control sample (FO) with a tendency to increase according to the interpolation polynomial and the correlation coefficient R^2 = 80 %. According to the hypothesis test (ANOVA), statistically, significant differences were observed with a confidence level of 95 %.

Otherwise, the density has the maximum value in the control sample (FO) and the minimum for the FPT treatment (averages between 0.79 $g.cm^{-3}$ and 0.32 $g.cm^{-3}$), with an inverse trend proportional to the incorporation of MCC in the films according to the interpolation polynomial and the correlation coefficient R^2 = 63 %, observing statistically significant differences with a confidence level of 95 %.

Air Permeability

The air permeability in the films resulted in averages above 1800 $s/100cm^3$, a value that, according to the standard TAPPI 460-om:2016 (TAPPI, 2016c), characterizes the material as impermeable.

X-Ray Diffraction

In Figure 4 the crystalline peaks for the different treatments are shown. All samples exhibited peaks 002 $22°\leq\theta\leq23°$ and IAM between $18°\leq\theta\leq19$, which is characteristic of type I cellulose, also known as native cellulose, which forms its structure by repeating β units (1-4) D-glucopyranose (Rol et al., 2019).

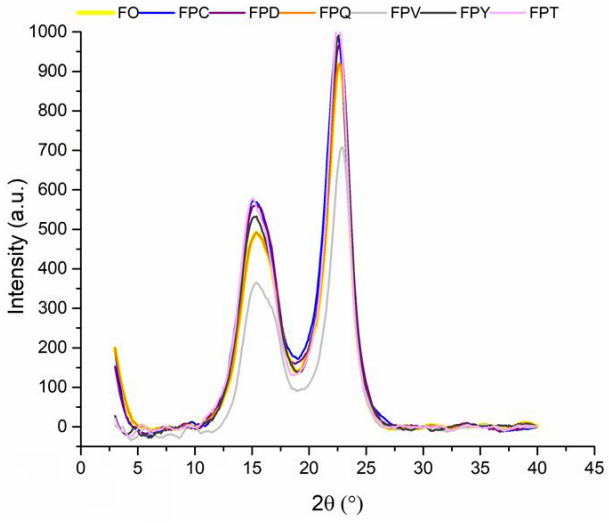

Figure 4. X-ray diffractogram for films.

Using the Segal method (Segal et al., 1959), the percentage of crystalline cellulose in the samples was calculated, estimating the difference between the intensity of the most significant crystalline peak (plane 002) and the minimum intensity between the two peaks.

Table 2. Segal index of films.

Sample	CI (%)
FO	76.91
FPC	77.74
FPD	78.90
FPQ	78.13
FPV	78.99
FPY	81.19
FPT	82.28

A maximum value of 82.28 % was observed for the FPT film (sample with the highest incorporation of MCC) and a minimum value of 76.91 % for the control sample (FO), with an increasing trend according to the interpolation polynomial and the correlation coefficient R^2 = 86%.

Chemical characterization

Zeta Potential

A value of -29.38 mV was observed for the FPT film (sample with the highest percentage of MCC addition) and a value of -17.60 mV for the film without MCC (control sample FO), with an increasing tendency according to the interpolation polynomial and the correlation coefficient R^2 = 83 %. In addition, it was observed that the samples had values with reduced dispersion (between the samples) that are evidenced in CV (%) less than 10 %, characteristic of homogeneous samples. In Table 3, the average zeta potential values obtained can be detailed.

Table 3. Zeta potential (mV) of suspensions.

Sample	Average
FO	-17.60a (4.5)
FPC	-21.12b (7.3)
FPD	-17.82a (2.3)
FPQ	-21.53b (6.0)
FPV	-25.10c (3.2)
FPY	-25.21c (5.2)
FPT	-29.38d (4.2)

Equal letters represent statistically similar means (Tukey). Values between relatives are the percentage variation coefficients of the samples.

Fourier Transform Infrared Spectroscopy (FTIR)

The films obtained from the suspensions were submitted to FTIR analysis to check functional groups' presence. As a result, it can be seen that the spectrum of all films is very similar and shows characteristic cellulose bands Figure 5.

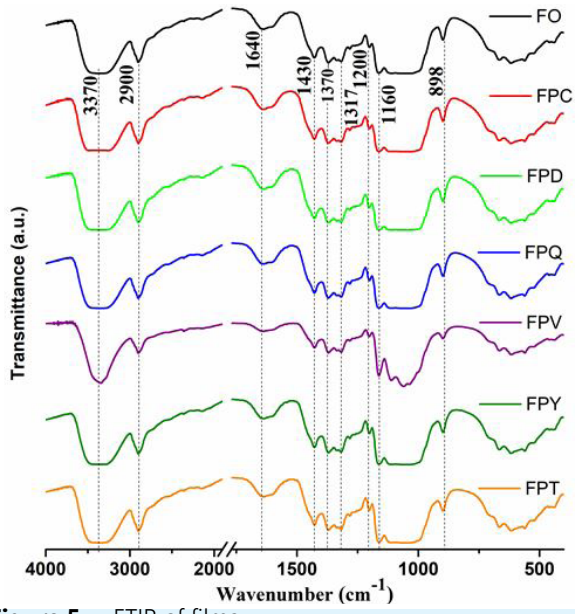

Figure 5. FTIR of films.

Thermal characterization of filmes

Thermogravimetric analysis (TGA)

In Figure 6, the thermal behavior of the studied samples is presented. An increase in the initial temperature was observed in films with higher amounts of MCC, from 226 °C (FO); 230°C (FPC); 232°C (FPD); 234°C (FPQ); 235°C FPV); 235 °C (FPY) to 237 °C (FPT), observing increases in the resistance to thermal degradation of the films.

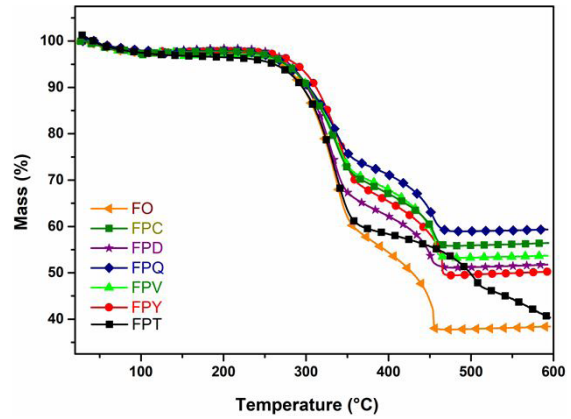

Figure 6. TGA curve of films.

DISCUSSIONS

Microstructural analysis of NFC/MCC suspensions and filmes

The TEM micrographs Figure 1a-g suggest the formation of a nano-lattice, produced by interactions and entanglement, mainly between the NFCs, which, as it is known, expose numerous hydroxyl groups along their chain.

Through the TEM micrographs, an analysis of diametric frequencies (Figure 2) of the structures of the materials of this study (vertical bars) and the average diameter of the fibers with their respective dispersions was performed. It can be seen that the control sample (FO) has a concentrated diameter ratio between 0-10 nm and 11-20 nm. As the concentration of MCC increases, there is an increase in the diameter of the structures in the frequency categories, decreasing the participation of the 0-10 nm category, and the 11-20 nm and 21-30 nm categories start to have greater participation. According to Hubbe et al. (2017), it can be explained by the formation of NFC and MCC aggregates because it makes sense to expect more tangles between the structures, especially when they are in an aqueous medium where elongated particles are forced to collide increasing the degree of agglomeration. Due to this, it can be expected that the cellulose-cellulose contact in a blend prepared under wet conditions can contribute to structural weaknesses as hydrogen bonds contribute to the bonding between fibers.

In SEM micrographs (Figure 3) of surface films, it was observed (when MCC started to be added – Figure 3b-g stress points or agglomerates (clusters) that occur when excess particles are added to the compositions (Espitia et al., 2013; Hubbe et al., 2017). According to Hubbe et al. (2017), nanocelluloses, when used as reinforcement in a polymer matrix, show maximum strength at a certain degree of reinforcement but a decrease in strength at high concentrations. The same author states that, thus, deterioration of higher reinforcement levels is sometimes attributed to the produced agglomerates; these agglomerates are generally groups of cellulose particles or fibers that in a structure can create weak points, mainly if there is air or direct contact between the cellulose particles without an intermediate polymer matrix. Pereira (2015) states that these stress points are prone to fracture, leading to a decrease in the mechanical properties of the nanofilm.

Physical characterization

Thickness and apparent density

The thickness of the films formed with the minor proportions of MCC was considerably smaller than those with more significant amounts. The coalescence of NFC and MCC particles can explain this, producing a less uniform and compact film. As the incorporation of MCC in the films increases, the rate of thickness is greater than the rate of increase in grammage due to the greater dimension of MCC in NFC matrix material.

Density is related to the porosity of the material; the more compacted the structures, the greater the number of hydrogen bonds and the denser the film; when they are denser, they have a positive influence on the mechanical properties of the films (Claro, 2017; Viana et al., 2019).

Air Permeability

Permeability, in turn, is directly related to the porosity and crystallinity of the material. A compact and little porous morphology generate resistance to the passage of air. Hubbe et al. (2017) reported that adding nanocellulose reinforcements to polymeric films can also reduce oxygen permeability due in part to the crystallinity of the nanocelluloses.

X-Ray Diffraction

As expected, adding MCC in different proportions in the NFC material increased the crystallinity index. That confirms the presence of amorphous regions in the NFC structure, different from MCC, which is produced using hydrolysis mechanisms with strong acids to remove the amorphous regions and preserve the crystalline ones. Therefore, it is hoped that the crystallinity index will always be higher for the MCC. The crystallinity of the MCC can vary between 65 % and 83 % (Manals; Penedo, 2011; Terinte, et al., 2011).

The increase in the crystallinity index in the films, proportional to the amounts of MCC added, produces an increase in the crystalline domains and favors the performance of the different properties of the evaluated materials.

According to Miranda (2015), the more cellulose present in the material, the more resistant it will be; however, the mechanical performance also depends on other structural parameters such as the number, length, and width of the unit cells, the lignin content present among others. In addition, Pereira (2015) states that the higher the crystallinity index in the materials, the more resistant they are to thermal degradation, while the crystalline regions are less susceptible to the action of heat.

It can be said that MCC has excellent potential for applications due to its high crystallinity, structural characteristics, and nature.

Hubbe et al. (2017) present a collection of information from several authors who found that NFC can have a crystallinity index between 60 % and 70 %. However, other values are reported in studies carried out on bleached pulp from *Eucalyptus sp* (Parize et al., 2017), with a crystallinity index of 61 %.

Chemical characterization

Zeta potential

An electrostatically stabilized nanosuspension is assigned values between -30 to +30 mV zeta potential (Jasmani and Adnan, 2017). However, particle aggregation can affect this stability, as the colloid tends to reduce the surface energy; the higher the load value (+or -), the more dispersed the particles and the greater the stability of the suspension (Savchenko and Velichko, 2019). In this way, the understanding of surface charges in formulations is essential because it is related to good dispersion of the particles.

The FO, FPC, FPD, and FPQ samples presented zeta potential in absolute value between 17 mV and 21 mV. In contrast, the FPV, FPY, and FPT samples presented zeta potential (in absolute value) between 25 mV and 29 mV. The samples in the first group can be easily agglomerated due probably to the more significant presence of the OH groups. In the second group, an increase in the zeta potential was observed, which can be explained, first, by the method of production of MCC, which occurs through acid hydrolysis with hydrochloric acid, resulting in a surface with negative charges, which contribute to a homogeneous dispersion of MCC, with less tendency to agglomerate and provide more excellent stability to the suspension. (Hindi, 2017; Pereira, 2015). The second aspect to consider is the size difference between nanofibrils and cellulose microcrystals, which probably influenced the different results obtained for zeta potential due to the possible entanglements of the structures (Palacios et al., 2019; Siqueira et al., 2009).

Fourier Transform Infrared Spectroscopy (FTIR)

Among the most significant bands found, the band of 3370 cm^{-1}, which refers to O-H vibrations, indicates the presence of cellulose (Dewes et al., 2018). Ciolacu et al., (2011) observed that this peak (characteristic of hydrogen bonds), when sharper and less intense, can occur due to intramolecular and intermolecular hydrogen bond divisions (Tozluoglu et al., 2017). The absorption band located at 2900 cm^{-1} refers to C-H stretching vibrations in the C-H, C-H_2, and C-H_3 functional groups. This displacement confirms the amorphous area's presence in the cellulosic samples (Ciolacu et al, 2011). The band located at 1640 cm^{-1} refers to water adsorption (Tozluoglu et al., 2017). At 1430 cm^{-1}, a band was observed, indicating vibrations in C-H_2, known as the crystallinity band (Lengowski, 2016). The bands found at 1370 cm^{-1} and 1317 cm^{-1} refer to deformations in the O-H, CH, and CH_2 functional groups, referring to cellulose (Tozlouoglu et al., 2017). The band observed at 1317 refers to the C-H twist and is responsible for the crystallinity. The peak observed at 1200 cm^{-1} provides similar information to the band at 3400 cm^{-1} (Tozlouoglu et al., 2017). The band observed at 1160 cm^{-1} refers to asymmetric vibrations and stretching in the C-O, C-C, and C-O-C bonds. The peak at 898 cm^{-1} provides information on the vibration of the anomeric carbon group of C1-H carbohydrate (Manals and Penedo, 2011).

Thermal characterization

Thermogravimetric analysis (TGA)

Three thermal events characteristic of lignocellulosic materials were observed: in the first event, the degradation of hemicelluloses occurs; in the second, the degradation of cellulose; and in the third, the decomposition of lignin begins (Sjostrom, 2013; Kawamoto et al., 2015). There were increasing variations in the initial temperature range (T_{onset})

with the increase of MCC; This result can be influenced by experimental conditions such as atmosphere or flow and heating rates in addition to the crystallinity, particle size, mass, or impurities, properties of cellulose (Leal et al., 2015).

The increase in the crystallinity index in the films, proportional to the amounts of MCC incorporated, produces an increase in the crystalline domains and favors the performance of the different properties of the materials. Other authors have observed that the higher the crystallinity index in the materials, the more excellent the resistance to thermal degradation due to them being less susceptible to the action of heat (Pereira, 2015; Lengowski et al., 2018). Thermal stability is considered a relevant characteristic for nanostructured films like effective reinforcement materials in different applications. The typical processing temperature of thermoplastic materials is above 200°C; therefore, nanostructured materials increasingly used as reinforcements should be evaluated regarding this property (Pereira, 2015).

CONCLUSION

Based on the results obtained in the study, it was possible to conclude the following; proportional increase in the diametric frequency of the structures in the suspensions was evidenced. Although thicknesses maintain a growing proportional relationship according to the incorporation of the MCC in the films, in terms of density, they present an inversely proportional relationship since the thickness growth taxa will be much higher than the grammature growth taxa. It was possible to control the grammature and statistically it did not change. According to Gurley's test, the films can be considered impermeable to air passage. An increase in the film's Segal index was observed according to the incorporation of MCC, equivalent to a percentage increase of 7%. It was obtained variations of the zeta potential values from unstable suspensions to suspensions close to stable. The films showed thermal stability greater than 220 °C, making them an alternative nanostructured and organic material for thermal integrity applications. The films produced may have the potential for various applications in the chemical sector and materials such as coatings, packaging, and the composition of a range of thermoplastic materials.

ACKNOWLEDGEMENTS

The authors thank Klabin and VIVAPUR JRS PHARMA for supplying raw materials. To the following Laboratories of the Federal University of Paraná for the technical support in the analyses; Pulp and paper; Wood chemistry; Center for Electron Microscopy CME; BioPol Laboratory; X-ray Diffraction Laboratory (Projects CT-INFRA 793/2004 AND 3080/2011). To the LQCE-ESALQ of the University of São Paulo and the Research Laboratory in Hybrid Materials of the Federal University of Sergipe. To the graduate program in Forest Engineering of the Federal University of Paraná and to the CNPq for financial support to the research.

AUTHORSHIP CONTRIBUTION

Project Idea: DAS, UK, ECL, ASA
Database: CF, LRLS, EAB
Processing: CF, LRLS, EAB, ASA
Analysis: CF, LRLS
Writing: CF
Review: DAS, UK, ECL, ASA

REFERENCES

CHU, Y; SUN, Y; WU, W; XIAO, H; Dispersion Properties of Nanocellulose: A Review. Carbohydrate Polymers, v. 250, 116892, 2020.

CIOLACU, D., FLORIN, C. AND VALENTIN, P. Amorphous cellulose – structure and characterization. Cellulose chemistry and technology, v. 45, p. 606–614, 2011.

CLARO, F.C. Elaboration and characterization of films from plant cellulose nanofibrils. 2017. 113 p. Thesis Federal University of Paraná, Curitiba

DEWES, I.; SCHEFFLER, G.; PAVAN, F.; MAZZOCATO, A. Infrared spectroscopy in the analysis of the chemical composition of different genotypes of Trifolium repens. 28 Brazilian Congress of Animal Science, anais. 2018.

DUSASTRE, V.; MARTIRADONNA. L. Materials for sustainable energy. Nat. Mater, v.16, p. 15-15, 2017.

ESPITIA, P. J. P., SOARES,N. F. F., TEÓFILO, R. F., COIMBRA, J. S. R., VITOR, D. M., BATISTA, R. A., FERREIRA, S. O., ANDRADE, N. J., MEDEIROS, E. A. A. Physical–mechanical and antimicrobial properties of nanocomposite films with pediocin and ZnO nanoparticles. Carbohyd Polym, v. 94, n. 1, 199-208, 2013.

FANG, Z.; HOU, G.; CHEN, C.; HU, L. Nanocellulose-based films, and their emerging applications. Current Opinion in Solid State and Materials Science, v. 23, n. 4, 100764, 2019.

FRENCH, A.D. Increment in evolution of cellulose crystallinity analysis. Cellulose, v. 27, p. 5445–5448, 2020.

FUENMAYOR, C.; Silva, D.A.; Klock, U.; Lengowski, E.; Andrade, A.S.; Bonfatti Júnior, E.A.; Trejo, J.; Nuñez, Y.; Palma, O.; Cademartori, P.H.G.; Muniz, G.I.B. Tribological behavior of cellulose nanostructured films. Surf. Topogr.: Metrol. Prop., v. 10, n. 3, 034001, 2022.

HAMEED, S.; WAGH A.S.; SHARMA, A.; PAREEK, V.; YU, Y.; JOSHI, J.B. Kinetic modelling of pyrolysis of cellulose using CPD model: effect of salt, J. Therm. Anal. Calorim, v. 147, p. 9763–9777, 2022.

HINDI, S. Microcrystalline Cellulose: The Inexhaustible Treasure for Pharmaceutical Industry. Nanoscience and Nanotechnology Research, v. 4, n. 1, p. 17–24, 2017.

HUANG, F.Y. Thermal properties and thermal degradation of cellulose tri-stearate (CTs), Polymers (Basel). v. 4, p. 1012–1024, 2012.

HUBBE, A.; FERRER, A.; TYAGI, P.; YIN, Y.; SALAS, C.; PAL, L.; ROJAS, O. Nanocellulose in thin films, coatings, and plies for packaging applications: A review. BioResources, v. 12 n. 1, p. 2143–2233, 2017.

JASMANI, L.; ADNAN, S. Preparation, and characterization of nanocrystalline cellulose from Acacia mangium and its reinforcement potential. Carbohydrate Polymers, v. 161, p. 166–171, 2017.

KAWAMOTO H.; WATANABE T.; SAKA S. Strong interactions during lignin pyrolysis in wood – A study by in situ probing of the radical chain reactions using model dimmers. Journal of Analytical and Applied Pyrolysis, v. 7, p. 630-7, 2015.

KHUYEN, V. T. K.; LE, D. V.; FISCHER, A. R., DORNACK, C. Comparison of Microplastic Pollution in Beach Sediment and Seawater at UNESCO Can Gio Mangrove Biosphere Reserve. Global Challenges v. 5, 2021.

KONSTANTINOVA, S.; SEMKINA, L.; ANIKUSHIN, B.; ZUIKOV, A.; GLAGOLEVA, O.; VINOKUROV, V. Natural Polymer Additives for Strengthening Packaging Materials. Chemistry and Technology of Fuels and Oils, v. 55, n. 5, p. 561–567, 2019.

L. JIANG, X. YUAN, G. ZENG, Z. WU, J. LIANG, X. CHEN, L. JIAN, H. WANG, H. WANG. Metal-free efficient photocatalyst for stable visible-light photocatalytic degradation of refractory pollutant Appl. Catal. B Environ., 221 (2018), pp. 715-725

LEAL, G.F.; RAMOS, L.A.; BARRETT, D.H.; CURVELO, A.A.S.; RODELLA, C.B. A thermogravimetric analysis (TGA) method to determine the catalytic conversion of cellulose from carbon-supported hydrogenolysis process, Thermochim. Acta. v. 616, p. 9–13, 2015.

LENGOWSKI, E. C. Formation and characterization of films with nanocellulose. 2016. 230 p. Thesis Federal University of Paraná, Curitiba.

LENGOWSKI, E. C. et al. Morphological, physical and thermal characterization of microfibrillated cellulose. Revista Árvore, v. 42, n. 1, 2018.

MANALS, E.; PENEDO, M. Thermogravimetric and differential thermal analysis of different plant biomass. Química Technology, v. 31, n. 2, p. 180–190, 2011.

MIRANDA, C. et al. Effect of surface treatments on the properties of bagasse of piaçava fiber Attalea funifera Martius. New Chemistry. v. 38, n. 2, p. 161-165, 2015.

MIRONOVA, M; MAKAROV, I; GOLOVA, I.; VINOGRADOV, M.; SHANDRYUK, G.; LEVIN, I. Improvement in Carbonization Efficiency of Cellulosic Fibres Using Silylated Acetylene and Alkoxysilanes, Fibers v. 7, n. 10, 2019.

MONTEIRO S.N.; CALADO, V.; MARGEM, F.M.; RODRIGUEZ, R.J.S. Thermogravimetric stability behavior of less common lignocellulosic fibers - A review, J. Mater. Res. Technol. v. 1, n. 3, p. 189–199, 2012.

NURAZZI, N.M.; ASYRAF, M.R.M.; RAYUNG, M.; NORRRAHIM, M.N.F.; SHAZLEEN, S.S.; RANI, M.S.A.; SHAFI, A.R.; AISYAH, H.A.; RADZI, M.H.M.; SABARUDDIN, F.A.; ILYAS, R.A.; ZAINUDIN, E.S.; ABDAN, K. Thermogravimetric analysis properties of cellulosic natural fiber polymer composites: A review on influence of chemical treatments, Polymers (Basel). v. 13, 2021.

PALACIOS, H.; HERNÁNDEZ, A., ESQUIVEL, M.; TORIZ, G.; ROJAS, O.; SULBARÁN, B. Isolation and Characterization of Nanofibrillar Cellulose from Agave tequilana Weber Bagasse. Advances in Materials Science and Engineering, 2019.

PARIZE, D. D. DA S., OLIVEIRA, J. E. DE, WILLIAMS, T., WOOD, D., AVENA BUSTILLOS, R. DE J., KLAMCZYNSKI, A. P., GLENN, G. M., MARCONCINI, J. M. AND MATTOSO, L. H. C. Solution blow spun nanocomposites of polylactic acid/cellulose nanocrystals from Eucalyptus kraft pulp. Carbohydrate Polymers, v.174, p.923–932, 2017.

PEREIRA, R. Characterization and applications of nanofibrillated (NFC) and nanocrystalline (CNC) celluloses. 2015. 90 p. Thesis Federal University of Viçosa, Viçosa

POTULSKI DC. Influence of nanocellulose on the physical and mechanical properties of primary and recycled paper from Pinus and Eucalyptus. 2016. 150 p. Thesis Federal University of Paraná, Curitiba

ROL, F.; BELGACEM, N.; GANDINI, A.; BRAS, J. Recent advances in surface-modified cellulose nanofibrils. Progress in Polymer Science, v. 88, p. 241–264, 2019.

SAVCHENKO, E.; VELICHKO, E. New techniques for measuring zeta-potential of colloidal system Proc. SPIE, Saratov Fall Meeting 2018: Optical and Nano-Technologies for Biology and Medicine, 110651U, 2019.

SEGAL, L.; CREELY, J.; MARTIN, E.; CONRAD, M. An empirical method for estimating the degree of crystallinity of native cellulose using the X-ray diffractometer. Textile Research Journal, v.29, n.10, p.786-794, 1959.

SIQUEIRA, G.; BRAS, J.; DUFRESNE, A. Cellulose whiskers versus microfibrils: Influence of the nature of the nanoparticle and its surface functionalization on the thermal and mechanical properties of nanocomposites. Biomacromolecules, v. 10, n. 2, p. 425–432, 2009.

SJÖSTRÖM E. Wood chemistry fundamentals and applications. New York: Academic Press. 2013.

SU, Y.; ZHAO, Y.; ZHANG, H.; FENG, X.; SHI, L.; FANG, J. Polydopamine functionalized transparent conductive cellulose nanopaper with long-term durability. J. Mater. Chem. C, v. 5, p. 573-581, 2017.

Technical Association of Pulp and Paper Industry (TAPPI) T402sp-94: standard conditioning and testing atmospheres for paper, board, pulp handsheets, and related products. Atlanta. 1994.

Technical Association of Pulp and Paper Industry (TAPPI) T412om-16: Moisture in Pulp, Paper, and Paperboard. Atlanta. 2016a.

Technical Association of Pulp and Paper Industry (TAPPI) T220sp-16: physical testing of pulp handsheets. Atlanta. 2016b.

Technical Association of Pulp and Paper Industry (TAPPI) T410om-19: Grammage of Paper and Paperboard (Weight per Unit Area). Atlanta. 2019.

Technical Association of Pulp and Paper Industry (TAPPI) T460om-16: Air Resistance of Paper (Gurley Method). Atlanta. 2016c.

TERINTE, N.; IBBETT, R.; SCHUSTER, K. C. Lenzinger Berichte, v. 89, p.118, 2011.

TOZLUOĞLU, A., POYRAZ, B., CANDAN, Z., YAVUZ, M. AND ARSLAN, R. Biofilms from micro/nanocellulose of NaBH4-modified kraft pulp. Bulletin of Materials Science, v.40, n.4, p.699–710, 2017.

TURBAK, F.; SNYDER, W. Microfibrillated cellulose, a new cellulose product: properties, uses, and commercial potential. Microfibrillated cellulose, a new cellulose product: properties, uses, and commercial potential, v. 37, p. 815–827, 1983.

VIANA, C.; GRACIELA, M.; ESTEVES, L. Physical and mechanical properties of nanostructured films obtained from Kraft pulp of Pinus sp. not bleached. Scientia Forestalis, v. 45, n. 116, p. 653–662, 2017.